

Modeling lasers and saturable absorbers via multilevel atomic media in the *Meep* FDTD software: Theory and implementation

Alexander Cerjan,¹ Ardavan Oskooi,² Song-Liang Chua,³ and Steven G. Johnson⁴

¹*Department of Physics, Pennsylvania State University, University Park PA 16802*

²*Simpetus LLC, San Francisco CA 94109*

³*DSO National Laboratories, Singapore*

⁴*Department of Mathematics, Massachusetts Institute of Technology, Cambridge MA 02139*

(Dated: July 24, 2020)

This technical note describes the physical model, numerical implementation, and validation of multilevel atomic media for lasers and saturable absorbers in *Meep*: a free/open-source finite-difference time-domain (FDTD) software package for electromagnetics simulation. Simulating multilevel media in the time domain involves coupling rate equations for the populations of electronic energy levels with Maxwell's equations via a generalization of the Maxwell–Bloch equations. We describe the underlying equations and their implementation using a second-order discretization scheme, and also demonstrate their equivalence to a quantum density-matrix model. The *Meep* implementation is validated using a separate FDTD density-matrix model as well as a frequency-domain solver based on steady-state *ab-initio* laser theory (SALT).

I. INTRODUCTION

One of the primary methods in computational electromagnetics is finite-difference time-domain (FDTD), which solves Maxwell's equations using a discretized temporal and spatial grid [1, 2]. Since its public release in 2006, the open source FDTD software package *Meep* (meep.readthedocs.io) has become a widely used tool for photonics research and development [3]. In its original implementation, *Meep* was limited to simulating either linear dielectric or conductive media, or instantaneous versions of the Pockels and Kerr effects. However, many important optical phenomena involve saturable nonlinear media, such as optical bistability and lasing, which has not been supported.

In this technical note, we outline *Meep*'s recent addition of saturable nonlinear media which enables the simulation of lasers and saturable absorbers. This is achieved by coupling Maxwell's equations (for the electromagnetic fields) to rate equations for atomic level populations via a polarization field, and co-evolving the resulting FDTD-discretized “Maxwell–Bloch” equations [1, 4–10]. This implementation is then validated against simulations of stable, multimode lasing calculated using the steady-state *ab-initio* laser theory (SALT) [11–14]. We also discuss how to derive the classical oscillator equations for a saturable nonlinear medium from the quantum mechanical equations of motion for an electron bound to an atom or molecule interacting with an electric field, i.e. the Bloch equations. Finally, we review different unit conventions in the literature.

II. EVOLUTION EQUATIONS FOR SATURABLE MEDIA

In saturable nonlinear media, the medium possesses a set of internal degrees of freedom, the occupations of its electronic states, that are coupled to the electromagnetic field through the dipole moments of possible transitions between these states. Mathematically, this coupling between the electric field and the saturable medium can be modeled either by using a classical oscillator equation for the polarization of the saturable medium, or via the evolution of the density matrix of the electronic states. In this section, we will first discuss the classical oscillator model, as these are the equations used in *Meep* for saturable media. Then, we will derive the equivalence between the classical oscillator equation and the density-matrix evolution equations.

A. Classical oscillator model

To model saturable nonlinear media, *Meep* uses a classical oscillator equation for the nonlinear portion of the polarization of the media,

$$\frac{d^2 \mathbf{P}_n}{dt^2} + \gamma_n \frac{d \mathbf{P}_n}{dt} + \left(\omega_n^2 + \left(\frac{\gamma_n}{2} \right)^2 \right) \mathbf{P}_n = -\Delta N_n(\mathbf{x}, t) \bar{\sigma}_n \mathbf{E}(\mathbf{x}, t), \quad (1)$$

coupled to a set of rate equations for the evolution of the populations within each electronic state,

$$\frac{\partial N_i(\mathbf{x})}{\partial t} = - \sum_j \Gamma_{ij} N_i(\mathbf{x}) + \sum_j \Gamma_{ji} N_j(\mathbf{x}) + \sum_n \Xi_{i,n} \left[\frac{1}{\omega_n \hbar} \mathbf{E}(\mathbf{x}, t) \cdot \left(\frac{\partial}{\partial t} + \frac{\gamma_n}{2} \right) \mathbf{P}_n(\mathbf{x}, t) \right]. \quad (2)$$

There are many subtle details about these equations, but let us first review the notation used in these equations.

$\mathbf{E}(\mathbf{x}, t) \in \mathbb{R}$ —electric field vector

$\mathbf{P}_n(\mathbf{x}, t) \in \mathbb{R}$ —nonlinear polarization density vector of the n th electronic transition

$N_i(\mathbf{x}, t) \in \mathbb{R}$ —population density of the i th electronic state across all atoms/molecules at \mathbf{x}

$\Delta N_n(\mathbf{x}, t) = N_i(\mathbf{x}, t) - N_j(\mathbf{x}, t)$ —inversion of the population of the n th dipole transition

$\omega_n \in \mathbb{R}$ —central transition frequency of the n th electronic transition

$\gamma_n \in \mathbb{R}$ —full-width half-maximum linewidth of the n th transition

$\Gamma_{ij} \in \mathbb{R}$ —non-radiative decay/pumping rate from state i to state j

$\bar{\sigma}_n \in \mathbb{R}^{(3 \times 3)}$ —coupling tensor between the electric field and nonlinear polarization

$\Xi_{i,n} = 0, \pm 1$ —only non-zero if state i is the upper (+1) or lower (−1) state in transition n

In Eqs. (1–2), there are two separate sets of indices, i, j which correspond to electronic states of the saturable medium, while n denotes a transition between two of these states that can potentially interact with the electric field. If E_i and E_j are the energies of these two electronic states, the corresponding central transition frequency is $\omega_n = (1/\hbar)(E_i - E_j)$. The two states linked by a transition are said to be ‘inverted’ if $N_i > N_j$ and $E_i > E_j$, i.e. that the higher energy state has a greater occupation than the lower energy state. In this case, the transition will yield spontaneous and stimulated emission. If the medium is not inverted, the transition will instead act as an absorber for incident electric fields with frequencies similar to the transition frequency, ω_n . In total, there are M partial differential equations which describe the evolution of the occupation of each of the electronic states, and N oscillator equations for each of the different nonlinear polarization fields.

In principle, every $i \neq j$ pair of states could have a non-zero dipole moment yielding a nonlinear polarization field, \mathbf{P}_n . However, in practice, many of these potential transitions can be ignored, either because the dipole matrix element is zero, meaning that $\bar{\sigma}_n = 0$, or because the two states have low occupations, usually because the non-radiative decay rates out of these states are much faster than the rate of stimulated emission, such that $\Delta N_n \approx 0$. This second condition can also occasionally occur because the two states are always approximately equally populated. In writing Eq. (2) the only transition terms (those in the square brackets) which are included in the evolution of electronic state i are those which actually couple to state i , such that $\Xi_{i,n} = \pm 1$, otherwise $\Xi_{i,n} = 0$.

The tensor $\bar{\sigma}_n$ represents the effective coupling strength between the nonlinear polarization field and the electric field. One can understand that this quantity must be a tensor because the dipole element between two electronic states (a vector),

$$\boldsymbol{\theta}_n = e \langle \psi_i | \hat{\mathbf{x}} | \psi_j \rangle, \quad (3)$$

in which $|\psi_i\rangle$ is the wavefunction of the i th electronic state and e is the charge of an electron, is not, in general, parallel to the electric field, while the induced nonlinear polarization is necessarily parallel to $\boldsymbol{\theta}_n$. Thus, it can be shown that

$$\bar{\sigma}_n = \left(\frac{2\omega_n}{\hbar} \right) \boldsymbol{\theta}_n^* \otimes \boldsymbol{\theta}_n. \quad (4)$$

In practice, $\bar{\sigma}_n$ can often be treated as a scalar, $\sigma_n = 2\omega_n |\boldsymbol{\theta}_n|^2 / \hbar$, as one is typically interested in understanding the response of a nonlinear medium in the regime where it maximally interacts with the electric field, i.e. when $\boldsymbol{\theta}_n \parallel \mathbf{E}$.

Finally, there are two additional terms in Eqs. (1–2) that are atypical when writing a classical oscillator model and associated population rate equations, $(\gamma_n/2)^2 \mathbf{P}_n$ on the left side of Eq. (1), and $(\gamma_n/2) \mathbf{P}_n$ on the right side of Eq. (2). Typically, these terms are approximated to zero on the assumption that $\omega_n \gg \gamma_n$. However, as will be shown in Sec. IV, these terms are necessary to find proper agreement with a density matrix model of saturable media, and so we include them here.

B. Implementation in Meep

Equations (1–2) are implemented in the *Meep* FDTD code via second-order-accurate centered-difference approximations. In such a discretization scheme, the key question is what spatial and temporal sampling points are used for

each variable. The electric field \mathbf{E} in *Meep* is discretized on a Yee grid [1], with the k -th component E_k sampled at points

$$E_{k,\mathbf{i}+\mathbf{e}_k/2}^m \stackrel{\text{def}}{=} E_k(m\Delta t, (\mathbf{i} + \mathbf{e}_k/2)\Delta x),$$

where $\mathbf{i} = (i_1, i_2, i_3) \in \mathbb{Z}^3$ is an integer coordinate of a grid point (Yee voxel vertex) and \mathbf{e}_k is the Cartesian unit vector in direction k . Compared to this grid, the electric polarization-density components $P_{n,k}$ are sampled at the *same* Yee grid points $P_{n,k,\mathbf{i}+\mathbf{e}_k/2}^m$. In contrast, the population-density components N_i are sampled as $N_{i,\mathbf{i}+\mathbf{o}/2}^m$ at the *center* $\mathbf{i} + \mathbf{o}/2$ of each Yee voxel, where $\mathbf{o} = (1, 1, 1)$, at the same time instant $m\Delta t$. This leads to the following equations to update \mathbf{P}_n and N_i at each timestep m of the FDTD simulations: given $\{N_i^{m-1}, \mathbf{P}_n^{m-1}, \mathbf{P}_n^m, \mathbf{E}^{m-1}\}$, *Meep* computes $\{\mathbf{E}^m, N_i^m, \mathbf{P}_n^{m+1}\}$ (in that order). The timestepping of the electromagnetic fields via Maxwell's curl equations [1] is essentially unmodified except for the coupling $\mathbf{E} = \mathbf{D} - \sum_n \mathbf{P}_n$ to the polarization field. \mathbf{E}^m is updated first because it depends only on \mathbf{P}_n^m ; then N_i^m is updated next because it depends on $\{N_j^{m-1}, \mathbf{E}^m, \mathbf{E}^{m-1}, \mathbf{P}_n^m, \mathbf{P}_n^{m-1}\}$ as described below in Eq. (6); then \mathbf{P}_n^{m+1} is computed from $\{N_i^m, \mathbf{P}_n^{m-1}, \mathbf{P}_n^m, \mathbf{E}^m\}$ via Eq. (7) below. (In consequence, *Meep* must store \mathbf{P}_n and \mathbf{E} from two consecutive timesteps, and can otherwise update its data in-place.)

First, we update N_j for each level $j = 1, \dots, L$ to obtain N_j^m from N_j^{m-1} . Let $\mathbf{N} \stackrel{\text{def}}{=} (N_1, \dots, N_L)$ denote the vector of population densities for all L levels being tracked in Eq. (2), and let $\mathbf{\Gamma}$ denote the $L \times L$ matrix of the Γ_{ij} transition rates. Let $w_j^{m-1/2}$ denote the rate of work being done on (or by) level j in Eq. (2) evaluated at time $(m-1/2)\Delta t$ for each voxel center $\mathbf{i} + \mathbf{o}/2$:

$$w_{j,\mathbf{i}+\mathbf{o}/2}^{m-1/2} \stackrel{\text{def}}{=} \sum_n \frac{\Xi_{i,n}}{\omega_n \hbar} \left[\frac{\mathbf{E}^{m-1} + \mathbf{E}^m}{2} \cdot \left(\frac{\mathbf{P}_n^m - \mathbf{P}_n^{m-1}}{\Delta t} + \frac{\gamma_n}{2} \frac{\mathbf{P}_n^{m-1} + \mathbf{P}_n^m}{2} \right) \right]_{\mathbf{i}+\mathbf{o}/2}. \quad (5)$$

Note that we must average timesteps m and $m-1$ to obtain the electric and polarization fields at timestep $m-1/2$ to second-order accuracy, while $\partial/\partial t$ is also computed by a second-order center-difference approximation around $m-1/2$. The $[\dots]_{\mathbf{i}+\mathbf{o}/2}$ term denotes the spatial averaging required to compute the dot product at the voxel center $\mathbf{i} + \mathbf{o}/2$ to second-order accuracy. That is, for each component k we first compute the corresponding dot-product term $E_k P_{n,k}$ at the Yee grid point $\mathbf{i} + \mathbf{e}_k$, and then we average four neighboring Yee-grid points to obtain the value at the center of the voxel. Let $\mathbf{w} \stackrel{\text{def}}{=} (w_1, \dots, w_L)$ denote a vector of these work values. The second-order discretized Eq. (2) for \mathbf{N} is then

$$\left[\frac{\mathbf{N}^m - \mathbf{N}^{m-1}}{\Delta t} \right]_{\mathbf{i}+\mathbf{o}/2} = (\mathbf{\Gamma}^T - \mathbf{\Gamma}) \left[\frac{\mathbf{N}^m + \mathbf{N}^{m-1}}{2} + \mathbf{w}^{m-1/2} \right]_{\mathbf{i}+\mathbf{o}/2} \quad (6)$$

(resembling a Crank-Nicolson scheme). Equation (6) can be rearranged to solve for \mathbf{N}^m . (Note that this rearrangement will include the matrix $[I - \frac{\Delta t}{2}(\mathbf{\Gamma}^T - \mathbf{\Gamma})]^{-1}$, which is precomputed before timestepping begins.)

Second, we update \mathbf{P}_n to compute \mathbf{P}_n^{m+1} . From Eq. (1), we obtain the following center-difference discretization (supporting diagonal $\bar{\sigma}_n$ matrices):

$$\left[\frac{P_{n,k}^{m+1} - 2P_{n,k}^m + P_{n,k}^{m-1}}{\Delta t^2} + \gamma_n \frac{P_{n,k}^{m+1} - P_{n,k}^{m-1}}{2\Delta t} + \left(\omega_n^2 + \left(\frac{\gamma_n}{2} \right)^2 \right) P_{n,k}^m \right]_{\mathbf{i}+\mathbf{e}_k/2} = - \left[\overline{\Delta N_n^m} \bar{\sigma}_{n,k,k} E_k^m \right]_{\mathbf{i}+\mathbf{e}_k/2}, \quad (7)$$

where $\overline{\Delta N_n^m}$ denotes the population density difference (between the n -th transition's levels) averaged over the four neighboring voxel centers to obtain the value of ΔN_n at $\mathbf{i} + \mathbf{e}_k/2$ to second-order accuracy in Δx . Equation (7) can be solved for $P_{n,k}^{m+1}$ in order to update \mathbf{P}_n from the current (\mathbf{P}_n^m) and previous (\mathbf{P}_n^{m-1}) polarization timesteps, along with the current electric field (\mathbf{E}^m) and population densities (\mathbf{N}^m).

Recall that *Meep* divides the simulation domain into rectilinear “chunks” in order to divide the simulation over multiple processors and other reasons [3]. The fact that the population densities \mathbf{N} must be averaged over neighboring voxels in order to obtain the value at the correct Yee grid point for Eq. (7) means that, in a parallel simulation, the population densities must be communicated between chunks at their boundaries before each timestep. Similarly, the polarization fields must be communicated along the boundaries (along with the electric fields [3]) to perform the averaging in Eq. (6). This synchronization step allows chunks to use the current populations and polarizations from neighboring chunks in order to update polarizations and populations, respectively, for points on the chunk boundaries.

C. Density matrix model

Rather than assuming that the dynamics of the bound electrons of the saturable media can be modeled as a damped harmonic oscillator, it is instead possible to derive this directly beginning from a quantum mechanical model of the evolution of the saturable medium [6, 7, 15],

$$\partial_t \hat{\rho} = \frac{-i}{\hbar} [\hat{H}_0 + \hat{H}_I, \hat{\rho}]. \quad (8)$$

Here, $\hat{\rho}$ is the density matrix of an individual atom/molecule of the medium, whose unperturbed Hamiltonian is \hat{H}_0 , such that $\hat{H}_0|\psi_i\rangle = E_i|\psi_i\rangle$, and the interaction Hamiltonian from the incident electric field is $\hat{H}_I = e\hat{\mathbf{x}} \cdot \mathbf{E}(\mathbf{x}, t)$. The evolution for individual density matrix elements in Eq. (8) can be rewritten and simplified as

$$\partial_t \rho_{ij} = -i\omega_{ij}\rho_{ij} - \frac{i}{\hbar} \sum_k^M (\boldsymbol{\theta}_{ik}\rho_{kj} - \rho_{ik}\boldsymbol{\theta}_{kj}) \cdot \mathbf{E}(\mathbf{x}, t), \quad (9)$$

in which we are using $\boldsymbol{\theta}_{ij} = e\langle\psi_i|\hat{\mathbf{x}}|\psi_j\rangle$.

The density matrices of individual atoms/molecules can then be linked to the total macroscopic polarization field as

$$\sum_n \mathbf{P}_n(\mathbf{x}, t) = - \sum_\alpha \delta(\mathbf{x} - \mathbf{x}^{(\alpha)}) \text{Tr}[\hat{\rho}^{(\alpha)} e\hat{\mathbf{x}}_\alpha], \quad (10)$$

in which $\mathbf{x}^{(\alpha)}$ and $\hat{\rho}^{(\alpha)}$ are the position and density matrix of atom α . It is also convenient to define the positive frequency polarization component of an individual transition,

$$\mathbf{p}_n^+(\mathbf{x}, t) = - \sum_\alpha \delta(\mathbf{x} - \mathbf{x}^{(\alpha)}) \rho_{ij}^{(\alpha)} \boldsymbol{\theta}_{ji} \equiv - \sum_\alpha \delta(\mathbf{x} - \mathbf{x}^{(\alpha)}) \rho_{ij}^{(\alpha)} \boldsymbol{\theta}_n^*, \quad (11)$$

which is related to the classical polarization fields as $\mathbf{P}_n = 2\text{Re}[\mathbf{p}_n^+]$, as well as

$$N_i(\mathbf{x}, t) = \sum_\alpha \delta(\mathbf{x} - \mathbf{x}^{(\alpha)}) \rho_{ii}^{(\alpha)}(t). \quad (12)$$

Given these definitions, we can rewrite Eq. (9) specifically for the occupations,

$$\partial_t N_i = \sum_{j \neq i}^M \Gamma_{ji} N_j - \sum_{j \neq i}^M \Gamma_{ij} N_i + \frac{2}{i\hbar} \sum_n^{N_T} \Xi_{i,n} \text{Im}[\mathbf{p}_n^+] \cdot \mathbf{E}, \quad (13)$$

and the polarization components,

$$\partial_t \mathbf{p}_n^+(\mathbf{x}, t) = - \left(\frac{\gamma_n}{2} + i\omega_n \right) \mathbf{p}_n^+ - \frac{i(N_i - N_j)}{\hbar} \boldsymbol{\theta}_n^* (\boldsymbol{\theta}_n \cdot \mathbf{E}). \quad (14)$$

Here, we have added the phenomenological dephasing rates of the transition, γ_n , as well as the pumping and decay rates between the different electronic states, Γ_{ij} .

To make the final connection to the classical oscillator model, Eqs. (1-2), first note that from Eq. (14) and the definition of the classical polarization field, we can write

$$\begin{aligned} \partial_t \mathbf{P}_n &= 2\partial_t \text{Re}[\mathbf{p}_n^+] \\ &= 2 \left(\omega_n \text{Im}[\mathbf{p}_n^+] - \frac{\gamma_n}{2} \text{Re}[\mathbf{p}_n^+] \right) \end{aligned} \quad (15)$$

$$\frac{1}{\omega_n} \left(\partial_t + \frac{\gamma_n}{2} \right) \mathbf{P}_n = 2\text{Im}[\mathbf{p}_n^+], \quad (16)$$

which, upon substitution into Eq. (13), completes the derivation of Eq. (2). To derive Eq. (1), we take a second time

derivative of Eq. (15),

$$\begin{aligned}
\partial_t^2 \mathbf{P}_n &= \partial_t \left(2\omega_n \text{Im}[\mathbf{p}_n^+] - \frac{\gamma_n}{2} \mathbf{P}_n \right) \\
&= -\frac{\gamma_n}{2} \partial_t \mathbf{P}_n + 2\omega_n \left(-\frac{\gamma_n}{2} \text{Im}[\mathbf{p}_n^+] - \omega_n \text{Re}[\mathbf{p}_n^+] - \frac{N_i - N_j}{\hbar} \boldsymbol{\theta}_n^* (\boldsymbol{\theta}_n \cdot \mathbf{E}) \right) \\
&= -\frac{\gamma_n}{2} \partial_t \mathbf{P}_n + \left(-\frac{\gamma_n}{2} \left(\partial_t + \frac{\gamma_n}{2} \right) \mathbf{P}_n - \omega_n^2 \mathbf{P}_n - \frac{2\omega_n(N_i - N_j)}{\hbar} \boldsymbol{\theta}_n^* (\boldsymbol{\theta}_n \cdot \mathbf{E}) \right) \\
&= -\gamma_n \partial_t \mathbf{P}_n - \left(\omega_n^2 + \left(\frac{\gamma_n}{2} \right)^2 \right) \mathbf{P}_n - \frac{2\omega_n(N_i - N_j)}{\hbar} \boldsymbol{\theta}_n^* (\boldsymbol{\theta}_n \cdot \mathbf{E}), \tag{17}
\end{aligned}$$

which is the result. As can be seen, the “extra” terms discussed at the end of Sec. II A appear naturally in deriving the classical oscillator equations from a microscopic theory. As such, the implementation of saturable media in *Meep* retains these extra terms to ease comparison against other theories which may possess them.

III. NATURAL UNITS OF SATURABLE MEDIA

If the saturable medium only possesses a single relevant radiative transition, i.e. $N = 1$, it is possible to rewrite Eqs. (1–2) in a dimensionless form. To do so, we first identify the relevant time scale which dictates the dynamics of the non-radiative decay rates, Γ_{ij} , and denote this time scale as Γ_{ts} . Using this time scale, the natural units of the fields and populations are

$$\begin{aligned}
\mathbf{E}_{\text{NU}} &= \frac{|\theta|}{\hbar \sqrt{\Gamma_{\text{ts}} \gamma / 2}} \mathbf{E}, \quad (\text{Same relation for } \mathbf{P}) \\
N_{i,\text{NU}} &= \frac{2|\theta|^2}{\hbar \gamma} N_i,
\end{aligned}$$

and the classical oscillator equations can be written as

$$\frac{d^2 \mathbf{P}}{dt^2} + \gamma \frac{d\mathbf{P}}{dt} + \left(\omega_a^2 + \left(\frac{\gamma}{2} \right)^2 \right) \mathbf{P} = -\omega_a \gamma \Delta N(\mathbf{x}, t) \mathbf{E}(\mathbf{x}, t), \tag{18}$$

$$\left(\frac{1}{\Gamma_{\text{ts}}} \right) \frac{\partial N_i(\mathbf{x})}{\partial t} = - \sum_j \frac{\Gamma_{ij}}{\Gamma_{\text{ts}}} N_j(\mathbf{x}) + \sum_j \frac{\Gamma_{ji}}{\Gamma_{\text{ts}}} N_j(\mathbf{x}) + \Xi_i \mathbf{E}(\mathbf{x}, t) \cdot \left(\left(\frac{1}{\omega_a} \right) \frac{\partial}{\partial t} + \frac{\gamma}{2\omega_a} \right) \mathbf{P}(\mathbf{x}, t). \tag{19}$$

In these equations, we have dropped the subscript n as there is only a single radiative transition everywhere except $\omega_n \rightarrow \omega_a$, which is denoted as the ‘atomic’ frequency to avoid confusion with the frequency of the fields.

In the special case that a two-level saturable medium is being used, there is a preferred choice of time scale which can be derived by noting that the total occupancy density in both levels must sum to the total density of atoms/molecules [16], such that

$$\Gamma_{\text{ts}} = \Gamma_{12} + \Gamma_{21}, \tag{20}$$

and corresponds to the rate at which the inversion, $N_2 - N_1$, decays to its equilibrium value in the absence of any fields.

IV. VALIDATION

To verify that saturable media are correctly implemented in *Meep*, we simulate lasing in a one-dimensional Fabry-Pérot cavity and compare these results against an earlier FDTD implementation [17] of the density-matrix equations, (13) and (14), as well as a nonlinear frequency-domain algorithm for the steady-state lasing solution, SALT [11–14]. The cavity consists of a dielectric slab, $n = 1.5$, with a perfectly-reflecting mirror on one end and an open facet out of which light can escape on the other end. Confinement of the field inside the cavity is strictly due to Fresnel reflection at the interface. This dielectric cavity is filled with a saturable two-level medium, in which the lower electronic state is being pumped to the upper state at a faster rate than the upper state non-radiatively relaxes to the lower state, $\Gamma_{12} > \Gamma_{21}$. In dimensionless *Meep* units ($c/(2\pi a)$), we take the transition frequency to be $\omega_a = 40/(2\pi)$, $\gamma/2 = 4/(2\pi)$,

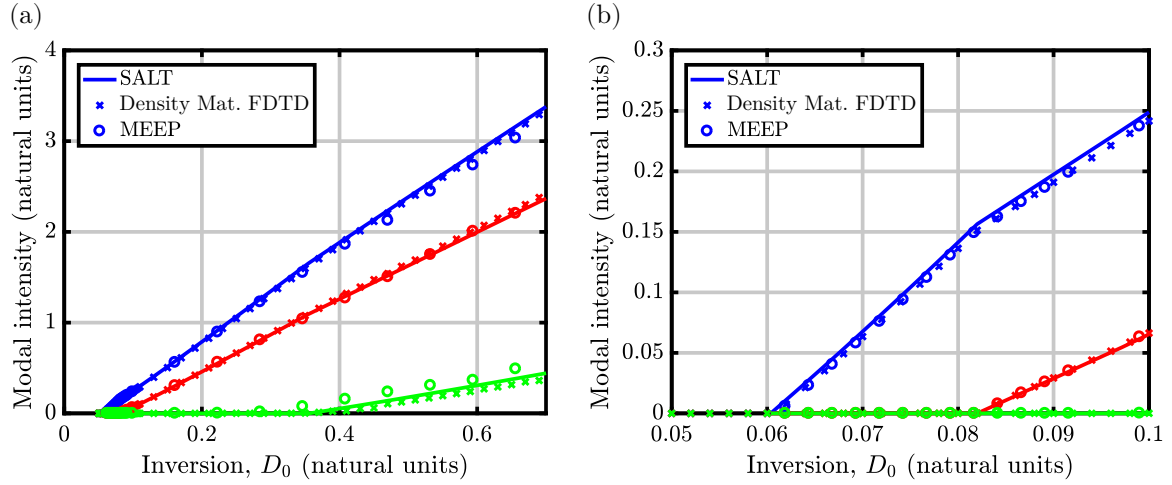


FIG. 1. (a) Comparison between the modal intensities found from FDTD simulations using *Meep*, the density matrix equations, and SALT through three lasing mode thresholds. The system has $\omega_a = 40/(2\pi)$, $\gamma/2 = 4/(2\pi)$, $\Gamma_{st} = 0.001/(2\pi)$, $\varepsilon = 1.5^2$, and $L = 1$. (b) Zoom-in on the region near the first two lasing thresholds.

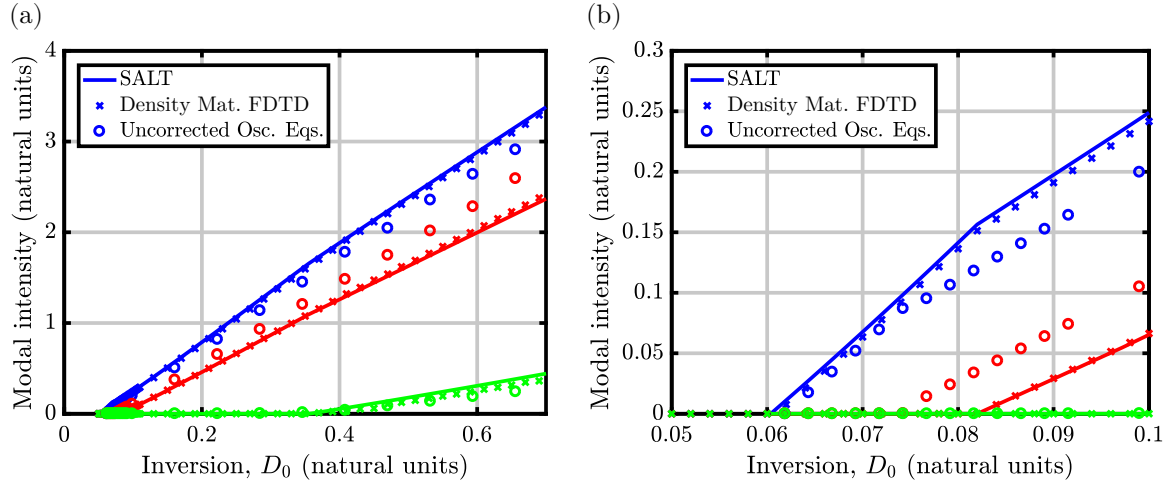


FIG. 2. (a) Comparison between the modal intensities found from FDTD simulations using *Meep* with the ‘uncorrected’ classical oscillator equations, the density matrix equations, and SALT through three lasing mode thresholds. The system has $\omega_a = 40/(2\pi)$, $\gamma/2 = 4/(2\pi)$, $\Gamma_{st} = 0.001/(2\pi)$, $\varepsilon = 1.5^2$, and $L = 1$. (b) Zoom-in on the region near the first two lasing thresholds.

$\Gamma_{ts} = 0.001/(2\pi)$, and assign the cavity a length of $L = 1$. In real units, if the lasing wavelength is $\lambda = 900$ nm, that corresponds to a cavity length of approximately $L \approx 6$ μm , which is an unphysically short cavity, but still useful for numerical comparisons. As a final note for this comparison, we use the inversion in the absence of the electric field, D_0 , as the effective pump parameter, which is defined in terms of the pumping and decay rates as

$$D_0 = \frac{\Gamma_{12} - \Gamma_{21}}{\Gamma_{12} + \Gamma_{21}} N_{\text{atom}}, \quad (21)$$

in which N_{atom} is the density of saturable atoms/molecules, $N_{\text{atom}} = N_1 + N_2$. As can be seen in Fig. 1, *Meep* simulations which are run sufficiently long for the system to reach its steady state agree with similar results from an independent FDTD based on the density matrix equations, as well as the steady-state lasing solution from SALT.

In addition, it is worth emphasizing here that the two terms which are typically approximated to zero in the classical oscillator equations, following the discussion from the end of Sec. II A, can play a significant role in understanding the details of the laser’s operation. Shown in Fig. 2 are simulations of the same laser system, but without these two extra terms in Eqs. (1–2), and as can be seen, there are significant deviations in the lasing thresholds and modal intensities.

V. USING SATURABLE MEDIA IN *MEEP*

In this section, we discuss how the parameters discussed in Sec. II A map to *Meep*'s Python API. In *Meep*, saturable media are defined using the `MultilevelAtom` class, which is a subclass of `E_susceptibilities`. There are two separate objects that one must specify to properly initialize `MultilevelAtom` – a set of radiative and non-radiative transitions that are both specified using `Transition`, and a set of initial populations of each of the electronic levels. The latter is straightforward, and is a list of the occupancies of the electronic states, $[N_1, N_2, \dots]$, at $t = 0$. To define a non-radiative transition, i.e. an element Γ_{ij} , the two levels must be specified, as well as the transition rate (in *Meep*'s frequency units of $c/(2\pi a)$),

```
meep.Transition(from_level=i, to_level=j, transition_rate= $\Gamma_{ij}$ )
```

If $i > j$, this represents a non-radiative decay rate, whereas if $i < j$ this represents a pumping rate, but both can be specified using `transition_rate`. To instead specify a radiative transition between two levels, which will implicitly initialize a corresponding non-linear polarization field \mathbf{P}_n , one must specify all of the necessary criteria for this transition,

```
meep.Transition(from_level=i, to_level=j, frequency= $\omega_n$ ,
                 gamma= $\gamma_n$ , sigma_diag=diag[ $\bar{\sigma}_n$ ])
```

In this case, it does not matter in what order you specify i and j , and again, both ω_n and γ_n are specified in *Meep*'s frequency units of $c/(2\pi a)$. Here, $\text{diag}[\bar{\sigma}_n]$ is specified as a `meep.Vector3`. If you have both a radiative and non-radiative transition between two levels, which is common because the upper level can be metastable, but not completely stable (as that would be a ground state), you can specify both processes in a single instance of `Transition`,

```
meep.Transition(from_level=i, to_level=j, transition_rate= $\Gamma_{ij}$ ,
                 frequency= $\omega_n$ , gamma= $\gamma_n$ , sigma_diag=diag[ $\bar{\sigma}_n$ ])
```

in which case the ordering of i and j does matter. At present, off-diagonal elements in $\bar{\sigma}_n$ are not supported, as discussed in Sec. II B.

Then, given a list of transitions, as well as a list of initial populations, one can define a multilevel atom susceptibility as

```
ml_atom = meep.MultilevelAtom(transitions=[list of transitions],
                               initial_populations=[ $N_1(t=0), N_2(t=0), \dots$ ])
```

which can now be added to any specification of a geometric object's material (or to the background medium of a simulation), as

```
material = meep.Medium(index= $n_{\text{cav}}$ , E_susceptibilities=[ml_atom])
```

Here, n_{cav} is the index of the linear response of the medium, independent of the non-linear saturable medium.

Given such a saturable-gain medium, in order to observe lasing one must initialize the electromagnetic field to a nonzero value (either by a short-lived current source or using the `initialize_field` function). Otherwise, there is no field to amplify into the lasing mode—the coupling between the electronic populations and the electromagnetic field in Eqs. (1–2) is zero when $\mathbf{E} = 0$. (In a physical system, nonzero fields are created by thermodynamic fluctuations.)

For the Python script used to generate the results in Sec. IV, see the [tutorial example](#) in the *Meep* user manual.

VI. CONCLUSION

In this technical note, we have described the physical model and numerical implementation of saturable media in *Meep*. Feature requests, bug reports, and suggestions for general improvements are welcome and can be made through either the user mailing list meep-discuss@ab-initio.mit.edu or as a Github issue via the source repository <https://github.com/NanoComp/meep>.

ACKNOWLEDGEMENTS

This work was supported in part by the U. S. Army Research Office through the Institute for Soldier Nanotechnologies (award W911NF-18-2-0048) as well as by the National Science Foundation (NSF) via Small Business Innovation Research (SBIR) Phase I and II awards 1647206 and 1758596. A.C. acknowledges the support of the US Office of

- [1] Allen Taflove and Susan C. Hagness, *Computational Electrodynamics: The Finite-Difference Time-Domain Method* (Artech House, 2005).
- [2] Allen Taflove, Ardavan Oskooi, and Steven G. Johnson, *Advances in FDTD Computational Electrodynamics: Photonics and Nanotechnology* (Artech, 2013).
- [3] Ardavan Oskooi, David Roundy, Mihai Ibanescu, Peter Bermel, J. D. Joannopoulos, and Steven G. Johnson, “Meep: A flexible free-software package for electromagnetic simulations by the FDTD method,” *Comput. Phys. Commun.* **181**, 687–702 (2010).
- [4] A.S. Nagra and R.A. York, “FDTD analysis of wave propagation in nonlinear absorbing and gain media,” *IEEE Trans. Antennas Propag.* **46**, 334–340 (1998).
- [5] Xunya Jiang and C. M. Soukoulis, “Time dependent theory for random lasers,” *Phys. Rev. Lett.* **85**, 70–73 (2000).
- [6] Shih-Hui Chang and Allen Taflove, “Finite-difference time-domain model of lasing action in a four-level two-electron atomic system,” *Opt. Express* **12**, 3827 (2004).
- [7] Yingyan Huang and Seng-Tiong Ho, “Computational model of solid-state, molecular, or atomic media for FDTD simulation based on a multi-level multi-electron system governed by Pauli exclusion and Fermi–Dirac thermalization with application to semiconductor photonics,” *Opt. Express* **14**, 3569 (2006).
- [8] Peter Bermel, Elefterios Lidorikis, Yoel Fink, and John D. Joannopoulos, “Active materials embedded in photonic crystals and coupled to electromagnetic radiation,” *Phys. Rev. B* **73** (2006).
- [9] Klaus Boehringer and Ortwin Hess, “A full time-domain approach to spatio-temporal dynamics of semiconductor lasers. II. Spatio-temporal dynamics,” *Prog. Quantum Electron.* **32**, 247–307 (2008).
- [10] Song-Liang Chua, Yidong Chong, A. Douglas Stone, Marin Soljačić, and Jorge Bravo-Abad, “Low-threshold lasing action in photonic crystal slabs enabled by fano resonances,” *Opt. Express* **19**, 1539 (2011).
- [11] Hakan E. Treci, A. Douglas Stone, and B. Collier, “Self-consistent multimode lasing theory for complex or random lasing media,” *Phys. Rev. A* **74**, 043822 (2006).
- [12] Hakan E. Treci, Li Ge, Stefan Rotter, and A. Douglas Stone, “Strong interactions in multimode random lasers,” *Science* **320**, 643–646 (2008).
- [13] Li Ge, Y. D. Chong, and A. Douglas Stone, “Steady-state *ab initio* laser theory: Generalizations and analytic results,” *Phys. Rev. A* **82**, 063824 (2010).
- [14] S. Esterhazy, D. Liu, M. Liertzer, A. Cerjan, L. Ge, K. G. Makris, A. D. Stone, J. M. Melenk, S. G. Johnson, and S. Rotter, “Scalable numerical approach for the steady-state *ab initio* laser theory,” *Phys. Rev. A* **90**, 023816 (2014).
- [15] Robert W. Boyd and Debbie Prato, *Nonlinear Optics*, 3rd ed. (Academic Press, Boston, 2008).
- [16] Alexander Cerjan, Yidong Chong, Li Ge, and A. Douglas Stone, “Steady-state *ab initio* laser theory for n -level lasers,” *Opt. Express* **20**, 474 (2012).
- [17] Alexander Cerjan, Y. D. Chong, and A. Douglas Stone, “Steady-state *ab initio* laser theory for complex gain media,” *Opt. Express* **23**, 6455 (2015).